2009년 8월

석사학위논문

# Prediction of a Reactor Core Power Peaking Factor Using Artificial Intelligence

조 선 대 학 교 대 학 원

원 자 력 공 학 과

배 인 호

# Prediction of a Reactor Core Power Peaking Factor Using Artificial Intelligence

- 인공지능을 이용한 원자로 출력첨두치 예측 -

2009년 8월 25일

조 선 대 학 교 대 학 원

원 자 력 공 학 과

배 인 호

# Prediction of a Reactor Core Power Peaking Factor Using Artificial Intelligence

지도교수 나 만 균

이 논문을 공학 석사학위신청 논문으로 제출함.

2009년 05월

조 선 대 학 교 대 학 원

원 자 력 공 학 과

배 인 호

# 배인호의 석사학위 논문을 인준함

위원장　조선대학교　교수　이 경 진　(인)

위　원　조선대학교　교수　김 진 원　(인)

위　원　조선대학교　교수　나 만 균　(인)

2009년　05월

## 조 선 대 학 교 대 학 원

# CONTENTS

# List of Tables



# List of Figures

# Abstract

## Prediction of a Reactor Core Power Peaking Factor Using Artificial Intelligence

배 인 호

지도 교수 : 나 만 균

조선대학교 일반대학원 원자력공학과

국부출력밀도(LPD)는 원자로 정상운전동안 핵연료와 핵연료피복경계면이 다양한 안전제한치 내에서 안전하게 운전되어지도록 정확하게 계산되어야한다. 안전성 관점에서 매우 중요한 노심의 가장 온도가 높은 부분에서의 LPD는 원자로 노심의 어떠한 위치에서의 LPD보다 중요한 데이터를 갖고 있다. 특히, 원자로가 운전되는 동안 LPD 모니터링은 핵연료 용융 현상을 방지하기 위해 중요한 것이다.

본 논문에서는 데이터 기반 인공지능 모델 중 두 가지 모델 (Fuzzy Neural Network, Support Vector Regression)을 출력첨두치(PPF) 예측을 위해 사용하였으며, 각각의 방법론을 고찰하였다. 그리고 Subtractive Clustering Method와 유전자 알고리즘을 사용함으로써 유용한 정보를 갖는 데이터를 얻고 제안된 알고리즘을 최적화시킬 수 있었다. 또한 성능 향상과 인공지능 방법의 잠재적인 Overfitting 문제를 해결하여 신뢰성 증진을 달성하기 위해 각각의 알고리즘을 적용했을 뿐만 아니라 서로 다른 모델을 결합함으로써 성능을 확인하였다.

예측성능을 비교해 본 결과 SVR 모델이 FNN 모델 결과에 비해 더 우수하다는 것을 알 수 있었으며, 이를 통해 실제 발전소내에서 출력첨두치(PPF)를 예측하기 위한 위 방법론이 적용가능하리라 기대된다.

# Ⅰ. Introduction

The Detailed 3-Dimensional (3D) core power distribution monitoring in operating nuclear power reactors is a prerequisite to ensure that various safety limits imposed on the fuel pellets and fuel clad barriers such as the local power density (LPD) and the departure from nucleate boiling ratio (DNBR) are not violated during reactor operation.

Local power density (LPD) should be calculated accurately to ensure that a number of safety limits imposed on the fuel pellets and fuel clad barriers are not violated during normal reactor operation. Since LPD at the hottest part of the nuclear core is of the major concern from safety perspective, the LPD at the hottest part of a hot nuclear fuel rod represents more important data than LPD at any other point of the nuclear reactor core. Especially, LPD monitoring in operating nuclear power reactors is important to prevent nuclear fuel rod melting.

The calculation of LPD and departure from nucleate boiling ratio (DNBR) constitutes two major functions of the core protection calculator system (CPCS) and the core operation limit supervisory system (COLSS) [1]. Both play an important role in the protection and monitoring systems of the optimized power reactor 1000 (OPR1000) developed in Korea. The COLSS is a program that runs in the plant monitoring system (PMS) computer, which helps plant operators to monitor the limiting conditions for operation (LCOs) specified in technical specifications. The COLSS monitors operating limits of the reactor core such as LPD and DNBR and provides related information to plant operators. However, the COLSS performs only monitoring functions regarding operating limits of the nuclear reactor core and does not provide protection features.

On the other hand, since CPCS provides protection of the nuclear reactor, it calculates faster than COLSS but produces more conservative values (lower DNBR

and higher LPD) than COLSS. COLSS periodically adjusts CPCS based on operating variables that are accurately calculated by COLSS, including power level, reactor coolant system (RCS) flow, etc.

LPD at the hottest part of the heated fuel rod, which can be expressed by the power peaking factor (PPF), is more important than LPD at any other point of the reactor core. DNBR studies have been extensively performed [2-8]. Meanwhile, little LPD research [9] has been conducted using artificial intelligence methods that have been successfully applied for solving a variety of engineering problems. Therefore, the objective of this thesis is to predict the PPF in the reactor core using measured signals of the RCS by applying Fuzzy Neural Network (FNN) and Support Vector Regression (SVR) models according to plant operating conditions.

The output and input data of the FNN and the SVR models are the PPF value in the reactor core and numerous operating conditions, which are characterized by reactor power, core inlet temperature, pressurizer pressure, coolant flow rate of the reactor core, axial shape index (ASI), in-core neutron flux, and a variety of control rod positions. The PPF value in the reactor core is calculated based on the developed FNN and SVR models using the above operating condition data as an input to FNN and SVR models. The proposed PPF calculation algorithm is verified by using nuclear and thermal data acquired from numerical simulations at Yonggwang nuclear power plant unit 3 (YGN-3).

# Ⅱ. Artificial Intelligence Methodology

## A. Fuzzy Inference Model

In fuzzy inference modeling, it is relatively easy to set up rough fuzzy rules for a target system by intuition if we understand its dynamics well. However, the task of fine-tuning the fuzzy rules to improve modeling performance is difficult. Therefore, propose an FNN that can embody fuzzy inference models are proposed. The proposed FNN provides functions for performing fuzzy inference. The functions can also be used to tune the parameters with respect to the shape of antecedent linguistic terms and the relative importance of rules.

The fuzzy inference system is constructed from a collection of fuzzy *if-then* rules. An artificial neural network is usually defined as a network composed of a large number of simple processors (neuron) that are massively interconnected, operate in parallel and learn from experience. A system that consists of a fuzzy inference system implemented in the framework of neural networks is usually called an adaptive network-based fuzzy inference system (ANFIS) or fuzzy neural networks [10]. In this work, the fuzzy neural network is used to predict the LPD as power peaking factor and the training of the fuzzy neural network is accomplished by a hybrid method combined with a backpropagation algorithm and a least-squares algorithm.

In the usual fuzzy inference system that is called the Mamdani fuzzy model [11], the *if* part is fuzzy linguistic and the *then* part is fuzzy linguistic, too, which requires a defuzzification process since the PPF estimation problem at hand has the input and output of real values. Therefore, a Takagi - Sugeno type [12] fuzzy model is used in which the *if* part is fuzzy linguistic, while the *then* part is crisp.

The Takagi-Sugeno type fuzzy inference system can be described as follows:

$$\begin{aligned} &if \quad x_1 \text{ is } A_{i1} \ AND \cdots \ AND \ x_m \text{ is } A_{im}, \\ &then \quad \hat{y}^i \text{ is } f^i(x_1, \cdots, x_m), \end{aligned} \tag{1}$$

where $x_j$ is the input variables to the fuzzy neural network ( $j = 1, 2, \cdots, m$ ; $m$ = the number of input variables), $A_{ij}$ the membership functions for the antecedent of the $i$-th rule and $j$-th input ($i = 1, 2, \cdots, n$ ; $n$ the number of rules), and $\hat{y}^i$ the output of the $i$-th rule. Usually $f^i(x_1, \cdots, x_m)$ is a polynomial in the input variables but it can be any function as long as it can appropriately describe the output of the fuzzy inference system within the fuzzy region specified by the antecedent of the rule. In this study, the symmetric Gaussian membership function is used. The output of an arbitrary $i$-th rule, $f^i$, consist of the first-order polynomial of inputs as given in Eq. (2)

$$f^i(x_1, \cdots, x_m) = \sum_{j=1}^{m} q_{ij} x_j + r_i \tag{2}$$

where $q_{ij}$ is the weighting value of the $j$-th input on the $i$-th rule output and $r_i$ is the bias of the $i$-th rule output. So the fuzzy inference rule expressed by Eqs. (1) and (2) is called a first-order Takagi-Sugeno type fuzzy rule.

The output of a fuzzy inference system with $n$ rules is a weighted sum of the consequent of all the fuzzy rules. The estimated output of the fuzzy inference system is given by:

$$\hat{y} = \sum_{i=1}^{n} \overline{w}^i f^i = \mathbf{w}^T \mathbf{q}, \tag{3}$$

where

$$\overline{w}^i = \frac{w^i}{\sum_{i=1}^{n} w^i},$$

$$w^i = \prod_{j=1}^{m} A_{ij}(x_j),$$

$$\mathbf{q} = [q_{11} \cdots q_{n1} \cdots \cdots q_{1m} \cdots q_{nm} \;\; r_1 \cdots r_n]^T,$$

$$\mathbf{w} = \left[\overline{w}^1 x_1 \cdots \overline{w}^n x_1 \cdots \cdots \overline{w}^1 x_m \cdots \overline{w}^n x_m \;\; \overline{w}^1 \cdots \overline{w}^n\right]^T$$

The superscript $i$ indicates that the parameters are related to the $i$-th rule.

For example, if the Takagi-Sugeno type fuzzy inference system is assumed to have two antecedents and two rules as follows:

$1^{st}$ rule: $if \;\; x_1$ is $A_{11} \;\; AND \;\; x_2$ is $A_{12}$, $then \;\; \hat{y}^1$ is $f^1(x_1, x_2) = q_{11}x_1 + q_{12}x_2 + r_1$,

$2^{nd}$ rule: $if \;\; x_1$ is $A_{21} \;\; AND \;\; x_2$ is $A_{22}$, $then \;\; \hat{y}^2$ is $f^2(x_1, x_2) = q_{21}x_1 + q_{22}x_2 + r_2$,

and in case triangular membership functions are used, Fig. 1 is an illustration of how the fuzzy inference system derives the overall output y when subjected to two crisp inputs $x_1$ and $x_2$. First, since the inputs are real-valued variables, a fuzzifier maps crisp points $x_1$ and $x_2$ in input universe of discourse $V \subset R^2$ to fuzzy sets in $V$. Then the degree of match $w^1$ and $w^2$ is found as, respectively

$$w^1 = \mu_{A_{11}}(x_1) \cdot \mu_{A_{12}}(x_2),$$

$$w^2 = \mu_{A_{21}}(x_1) \cdot \mu_{A_{22}}(x_2).$$

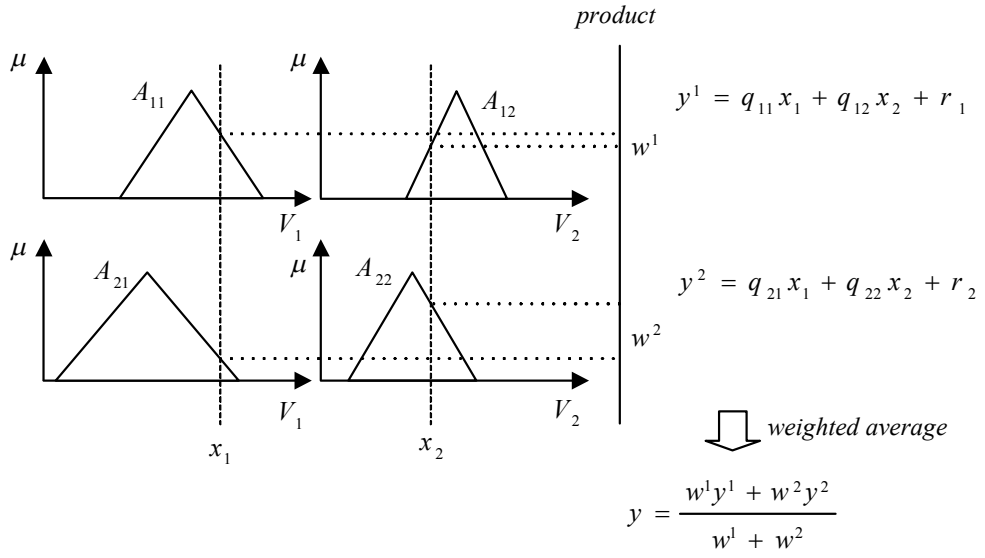


Fig. 1. A Takagi-Sugeno fuzzy inference system using algebraic product for fuzzy and operators.

The relative magnitude of the match $w^1$ and $w^2$ indicates the compatibility of each rule. In this study, algebraic product for fuzzy AND operator is used. Since each rule has a crisp output, the time-consuming defuzzification procedure is avoided and the overall output is obtained via the weighted average operator as shown in Fig.1. It is natural to optimize the membership functions $A_{ij}$ and consequent parameters $q_{ij}$ and $r_i$, which means that the fuzzy neural network should be trained.

The back-propagation algorithm that uses a gradient descent method is a general method for recursively training the fuzzy neural networks. The gradient descent method tunes the antecedent parameters (the center position of membership functions and their sharpness) so that a predefined objective function $E$ is minimized. In order to train an antecedent parameter $a_{ij}$, the following iterative calculation is used:

$$a_{ij}(t+1) = a_{ij}(t) - \eta_a \frac{\partial E}{\partial a_{ij}}|_t \tag{4}$$

where $E = \sum_{k=1}^{N} (y_k - \hat{y_k})^2$, i = 1, 2, ⋯, n, j = 1, 2, ⋯, m, t = 0, 1, 2, ⋯, and $\eta_a$ is a learning rate for a parameter $a$. The gradient descent method is very stable when the learning rate is small but susceptible to local minimum.

If the antecedent parameters of the fuzzy inference system are fixed by the backpropagation algorithm, the resulting fuzzy neural networks is equivalent to a series of expansions of some basis functions. This basis function expansion is linear in its adjustable parameters. Therefore, the least-squares method is used to determine the remaining parameters (consequent parameters $q_{ij}$ and $r_i$). If a total number of $N$ input-output training data are given, from Eq. (3) the consequent parameters are chosen to minimize the following cost function, which means that the sum of squared errors between the measured training data and the estimated values should be minimized:

$$J = \frac{1}{2} \sum_{k=1}^{N} (y_k - \hat{y}_k)^2 = \frac{1}{2} (\mathbf{y} - \hat{\mathbf{y}})^2 = \frac{1}{2} (\mathbf{y} - \mathbf{W}\mathbf{q})^2, \tag{5}$$

where

$$\mathbf{y} = [y_1 \; y_2 \cdots \; y_N]^T,$$

$$\hat{\mathbf{y}} = [\hat{y_1} \; \hat{y_2} \cdots \hat{y_N}]^T,$$

$$\mathbf{q} = [q_{11} \cdots q_{n1} \cdots \cdots \; q_{1m} \cdots q_{nm} \; r_1 \cdots r_n]^T,$$

$$\mathbf{W} = [w_1 \; w_2 \cdots \; w_N]^T,$$

$$\mathbf{w}_k = [\overline{w}^1 x_1 \cdots \overline{w}^n x_1 \cdots \cdots \overline{w}^1 x_m \cdots \overline{w}^n x_m \; \overline{w}^1 \cdots \overline{w}^n]^T$$

for $k$-th input data $(k=1,2,\cdots,N)$.

$\mathbf{y}$ is the output data vector, $\mathbf{q}$ is the parameter vector, and the matrix $\mathbf{W}$ includes the input data. The equation for minimizing the cost function is as follows:

$$\mathbf{y}=\mathbf{W}\mathbf{q}. \tag{6}$$

The fuzzy neural network output is represented by the $N\times(m+1)n$-dimensional matrix $\mathbf{W}$ and the $(m+1)n$-dimensional parameter vector $\mathbf{q}$. The parameter vector $\mathbf{q}$ in Eq. (6) is solved by using the pseudo-inverse of the matrix $\mathbf{W}$.

The value $\overline{w}^i$ represents the normalized compatibility grade of the $i$-th fuzzy rule and consists of the input data and the normalized membership function values. The vector $\boldsymbol{q}$ is called the consequent parameter vector. Fig. 2 describes the calculation procedure of the FNN model.

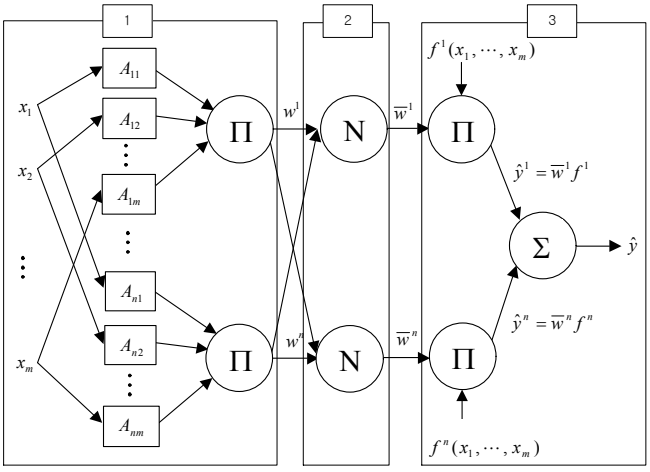


Fig. 2. A fuzzy neural network model

## B. Support Vector Regression (SVR)

Support vector regression (SVR) models are an alternative training method using a kernel function for an artificial neural network (ANN) where network weights are found by solving a quadratic programming problem with linear constraints rather than by solving a non-convex unconstrained minimization problem as in conventional neural network training. The SVR models use the hypothesis space of linear functions in multidimensional feature space. They are trained with a learning algorithm that originates from theoretical foundations of statistical learning theory and structural risk minimization (SRM).

Fig. 3 shows the SRM principle [10]. ANNs use conventional empirical risk minimization (ERM) principle to minimize approximation errors of the training data. On the other hand, the SVR model uses an SRM principle to minimize the upper bound of the expected risk [11]. The risk bound is the sum of the empirical risk and the confidence interval. The SVR model can be well applied to regression and classification problems. This thesis solves a typical regression problem to calculate the PPF value using various measured signals.

ERM methods minimize only the empirical risk at any cost whereas SRM methods finds the function $f^*$ that gives the smallest guaranteed risk $R(f^*)$ for the given data set. The empirical risk decreases with increasing capacity (with the index of the structure element, $h$), while the confidence interval increases. The smallest bound of the risk is achieved at some element of the structure as shown in Fig. 3. In Fig. 3, $h_k$ stands for the dimension of the set of functions of the learning machines. A structure on the set of functions is determined by the nested subsets of functions; $S_1 \subset S_2 \subset S_3 \subset \cdots$. Any element $S_k$ of structure has a finite dimension $h_k$. The difference in risk minimization leads to better generalization in SVR model than ANNs [10].

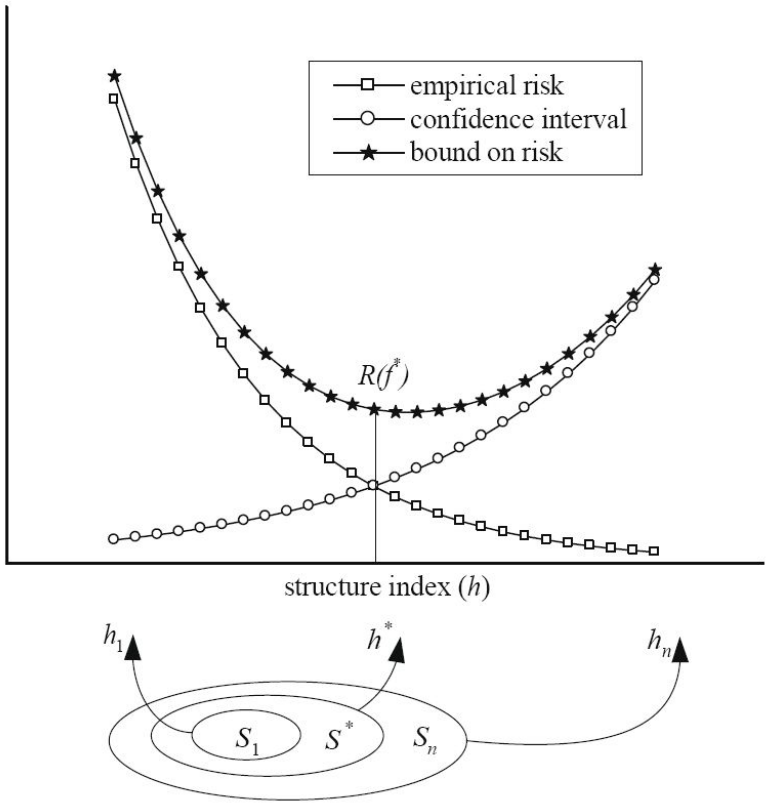


Fig. 3. Graphical representation of the SRM principle [10].

An SVR model learns a relationship between the input and the output from the training data set $\{(\mathbf{x}_i, y_i)\}_{i=1}^{N} \in R^m \times R$ where $\mathbf{x}_i$ is the input vector to the SVR model. The SVR model can be represented by [12]:

$$y = f(\mathbf{x}) = \sum_{i=1}^{N} w_i \phi_i(\mathbf{x}) + b = \mathbf{w}^T \boldsymbol{\phi}(\mathbf{x}) + b \tag{7}$$

where the function $\phi_i(\mathbf{x})$ is called the feature that is nonlinearly mapped from the input space $\mathbf{x}$, $\mathbf{w} = [w_1\ w_2\ \cdots\ w_N]^T$, and $\boldsymbol{\phi} = [\phi_1\ \phi_2\ \cdots\ \phi_N]^T$.

Eq. (7) is a nonlinear regression model because the resulting hyper-surface is a nonlinear surface hanging over the $m$-dimensional input space. However, after the input vectors $\mathbf{x}$ are mapped into vectors $\phi(\mathbf{x})$ of a multidimensional kernel-induced feature space, the nonlinear regression model is turned into a linear regression model in this feature space. The nonlinear function is learned using a linear learning machine where the learning algorithm minimizes a convex functional. The convex functional is expressed as the following regularized risk function, and the support vector weight $\mathbf{w}$ and bias $b$ are calculated by minimizing the following regularized risk function:

$$R_r(\mathbf{w}) = \frac{1}{2}\mathbf{w}^T\mathbf{w} + \lambda\sum_{i=1}^{N}|y_i - f(\mathbf{x})|_\epsilon \tag{8}$$

where

$$|y_i - f(\mathbf{x})|_\epsilon = \begin{cases} 0 & |y_i - f(\mathbf{x})| < \epsilon \\ |y_i - f(\mathbf{x})| - \epsilon & otherwise \end{cases} \tag{9}$$

The first term of Eq. (8) is a weight vector norm and the second term is an approximation error. The constant $\lambda$ which is one of the user-specified parameters is known as the regularization parameter. The regularization parameter determines the trade-off between the approximation error and the weight vector norm. An increase in the regularization parameter penalizes larger errors, which leads to a decrease of the approximation error. This can also be easily achieved by increasing the weight vector norm. However, an increase in the weight vector norm does not ensure good generalization of the SVR model. These parameters are determined from many simulations of the proposed SVR model.

$|y_i - f(\mathbf{x})|_\epsilon$ which uses another user-specified parameter ε is called the ε-insensitive loss function [10]. The loss equals zero if the predicted value $f(\mathbf{x})$ falls within the insensitivity zone ε, that means that the predicted value is inside the insensitivity zone. For all other predicted points outside the insensitivity zone, the

loss is equal to the magnitude of the difference between the predicted value and ε, which is represented by the parameters $\xi_i$ and $\xi_i^*$ [refer to Fig. 5]. The parameters $\xi_i$ and $\xi_i^*$ are positive values. These measure the cost of the errors on the training points and become zero for all points inside the insensitive ε-tube. Increasing the insensitivity zone ε means reducing the requirements for the accuracy of the approximation and decrease of the number of support vectors, leading to data compression. In addition, increasing the insensitivity zone ε has filtering effects on heavily noisy data.

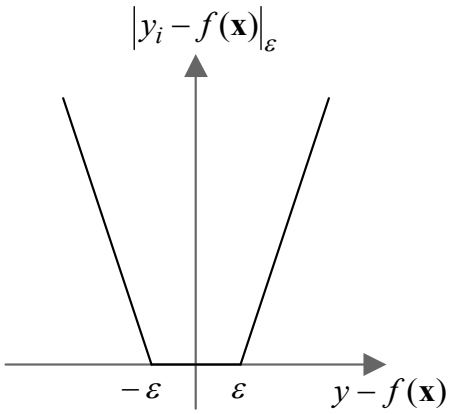


Fig. 4. Linear ε-insensitive loss function.

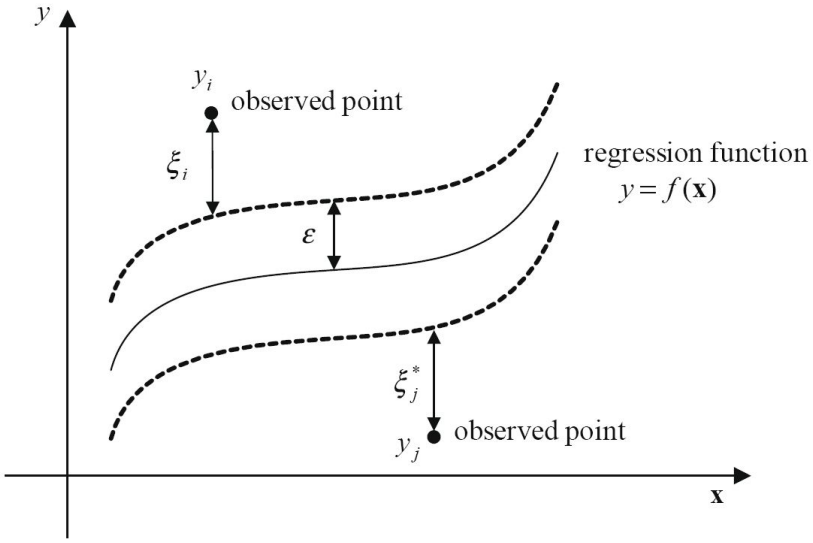


Fig. 5. Insensitive ε-tube and slack variables $\xi_i$ and $\xi_j^*$ for the SVR Model [13].

The regularized risk function of Eq. (8) is converted into the following constrained risk function:

$$R_c(\mathbf{w},\xi,\xi^*) = \frac{1}{2}\mathbf{w}^T\mathbf{w} + \lambda\sum_{i=1}^{N}(\xi_i + \xi_i^*) \tag{10}$$

subject to constraints

$$\begin{cases} y_i - \mathbf{w}^T\boldsymbol{\phi}(\mathbf{x}) - b \le \epsilon + \xi_i, & i = 1,2,\cdots,N \\ \mathbf{w}^T\boldsymbol{\phi}(\mathbf{x}) + b - y_i \le \epsilon + \xi_i^*, & i = 1,2,\cdots,N \\ \xi_i,\ \xi_i^* \ge 0, & i = 1,2,\cdots,N \end{cases} \tag{11}$$

where

$$\boldsymbol{\xi} = [\xi_1 \ \ \xi_2 \ \ \cdots \ \ \xi_N]^T,$$

$$\boldsymbol{\xi}^* = [\xi_1^* \ \ \xi_2^* \ \ \cdots \ \ \xi_N^*]^T.$$

The parameter $\xi_i$ and $\xi_i^*$ are slack variables representing upper and lower constraints on the outputs of the system, respectively, and they are positive values (refer to Fig. 5). The constrained optimization problem of Eq. (10) can be solved by applying the Lagrange multiplier technique to Eqs. (10) and (11) and then by using a standard quadratic programming techinque. Finally, the regression function of Eq. (7) becomes

$$y = f(\mathbf{x}) = \sum_{i=1}^{N} (\alpha_i - \alpha_i^*) K(\mathbf{x}, \mathbf{x_i}) + b, \tag{12}$$

where $K(\mathbf{x}_i, \mathbf{x}) = \boldsymbol{\phi}^T(\mathbf{x_i})\boldsymbol{\phi}(\mathbf{x})$ is called the kernel function. In this thesis, SVR models use a radial basis kernel function, $K(\mathbf{x}_i, \mathbf{x}) = \exp\left(-\frac{(\mathbf{x}-\mathbf{x}_i)^T(\mathbf{x}-\mathbf{x}_i)}{2\sigma^2}\right)$. A number of coefficients $\alpha_i - \alpha_i^*$ have non-zero values and the corresponding training data points are called support vectors (SVs) that have approximation errors equal to or larger than the error level ε.

# Ⅲ. Optimization of Data-based Models

## A. Model Optimization

The SVR and FNN models are designed by learning from given data and should be optimized to maximize the prediction performance. The performance of the SVR model depends heavily on the three types of design parameters such as the insensitivity zone $\epsilon$, the regularization parameter $\lambda$, and the kernel function parameters. Therefore, these parameters must be optimized by a genetic algorithm in order to maximize the performance of the SVR model. If these parameters are

not optimized, the model can be inferior in performance.

Genetic algorithm is less susceptible to being stuck at local minima than conventional search methods since genetic algorithms start from many points simultaneously climbing many peaks in parallel. Also, the genetic algorithm is the most useful method to solve optimization problems with multiple objectives. The genetic algorithm is used to optimize the insensitivity zone $\epsilon$, the regularization parameter $\lambda$, and the sharpness $\sigma$ of the radial basis kernel function used in this thesis that is expressed as follow:

$$K(\boldsymbol{x}_i, \boldsymbol{x}) = \exp\left(-\frac{(\boldsymbol{x}-\boldsymbol{x}_i)^T(\boldsymbol{x}-\boldsymbol{x}_i)}{2\sigma^2}\right). \tag{13}$$

The genetic algorithm requires a fitness function that assigns a score to each chromosome (candidate solution) in the current population, and maximizes the fitness function value. The fitness function evaluates the extent to which each candidate solution is suitable for specified objectives. A root mean square (RMS) error and a maximum error can be a measure of the prediction performance of the SVR model. However, the minimization of the errors only may induce the overfitting in these models, which means that these models is fitted well for only a specific data set (training data) but is not fitted for another data set.

In usual learning problems, the proposed model is trained using exemplary situations (training data) for which the desired output is already known. It is assumed that the model will also be able to predict the correct output for other situations, thus generalizing to situations not presented during training. But especially in cases where learning was performed too long or where training data are rare, the proposed model may adjust to very specific random features of the training data, which have no causal relation to the target function. In this process of overfitting, the performance on the training data still increases while the performance on the test data becomes worse.

Regularization has been applied successfully to numerous machine learning problems including the avoidance of overfitting [14]. It is a well-known method for the treatment of mathematically ill-posed problems. In this thesis, through the regularization that these models are optimized independently by using a data set independent of the training data, this kind of overfitting problems can be overcome. Therefore, the acquired data are divided into three types of data sets such as the training data, the optimization data, and the test data. The training data are used to solve the coefficients $\alpha_i - \alpha_i^*$ and the bias $b$ in Eq. (12) of the SVR models.

In case of FNN, the training data are used to solve the antecedent parameters of the FNN model. The optimization data are used in optimizing the SVR and FNN models by using another independent data set to improve generalization capability of these models. The test data are used to independently verify the developed models. The specified multiple objectives are to minimize the RMS error along with the small maximum error:

$$F = \exp(-\mu_1 E_1 - \mu_2 E_2 - \mu_3 E_3 - \mu_4 E_4) \tag{14}$$

where $\mu_1$, $\mu_2$, $\mu_3$ and $\mu_4$ are the weighting coefficients. $E_1$ and $E_2$ indicate the root mean squared error for the training data and the optimization data, respectively. $E_3$ and $E_4$ indicate the maximum error for the training data and the optimization data. These parameters are defined as follows:

$$E_1 = \sqrt{\frac{1}{N_t}\sum_{i=1}^{N_t}(y_i^t - \hat{y}_i^t)^2}\,, \tag{15}$$

$$E_2 = \sqrt{\frac{1}{N_o}\sum_{i=1}^{N_o}(y_i^o - \hat{y}_i^o)^2}\,, \tag{16}$$

$$E_3 = \max\left\{y_i^t - \hat{y}_i^t\right\}, \tag{17}$$

$$E_4 = \max\left\{y_i^o - \hat{y}_i^o\right\}. \tag{18}$$

The variables $y_i$ and $\hat{y}_i$ denote the measured output and the output predicted by the SVR and FNN models, respectively. The number $N$ represents the number of the training data. The superscripts, $t$ and $o$, indicate the training data and the optimization data, respectively, and $N_t$ and $N_o$ represent the numbers of the training data and the optimization data.

In the FNN case, if the antecedent parameters are fixed by the genetic algorithm, the output of the resulting FNN model can be described as a series of expansions of some basis functions. The basis function expansion is linear in its adjustable parameters, as shown in Eq. (3), because $\mathbf{w}^T$ is known by the genetic algorithm. Thus, the least squares method can be used to determine the consequent parameters. The consequent parameter $\mathbf{q}$ was chosen to minimize the following cost function, including the squared error between the target output $\mathbf{y}$ and the estimated output $\hat{\mathbf{y}}$:

$$J = \sum_{k=1}^{N_t} (\mathrm{y} - \hat{\mathrm{y}})^2 = \sum_{k=1}^{N_t} (\mathrm{y} - \mathbf{w}^T\mathbf{q})^2 = \frac{1}{2}(\mathbf{y} - \hat{\mathbf{y}})^2, \tag{19}$$

where

$$\mathbf{y} = [y_1\ y_2 \cdots\ y_N]^T \quad \text{and} \quad \hat{\mathbf{y}} = [\hat{y}_1\ \hat{y}_2 \cdots\ \hat{y}_N]^T.$$

The solution for minimizing the above cost function can be obtained by

$$\mathbf{y} = \hat{\mathbf{y}} = \mathbf{W}\mathbf{q}, \tag{20}$$

where

$$\mathbf{W} = [\mathrm{w}_1\ \mathrm{w}_2 \cdots\ \mathrm{w}_N]^T.$$

To solve the parameter vector $\mathbf{q}$ in Eq. (20), we should ensure that the matrix $\mathbf{W}$ is invertible but not usually a square matrix. We can easily solve the parameter

vector $\mathbf{q}$ in Eq. (20) by using the pseudo-inverse of the $\mathbf{W}$ matrix as follows:

$$\mathbf{q} = (\mathbf{W}^T\mathbf{W})^{-1}\mathbf{W}^T\mathbf{y}. \tag{21}$$

The parameter vector $\mathbf{q}$ can be calculated with a series of $N$ input/output data pairs prepared for the training data.

## B. Data Selection

To increase the learning efficiency and performance, the proposed models should be trained well by using informative datas. The training data set is selected using a subtractive clustering (SC) scheme [16]. Fig. 6 shows data clusters and their centers (indicated as '+' signs) as an example of simple two-dimensional data. An SVR model can be well trained by using data that include a lot of information. Since the nuclear reactor system is very complex and the acquired data should cover the entire range of operating conditions, it is expected that input and output training data sets have a lot of clusters and the data at the cluster centers is more informative than the neighboring data. The cluster centers are used as a training data set.

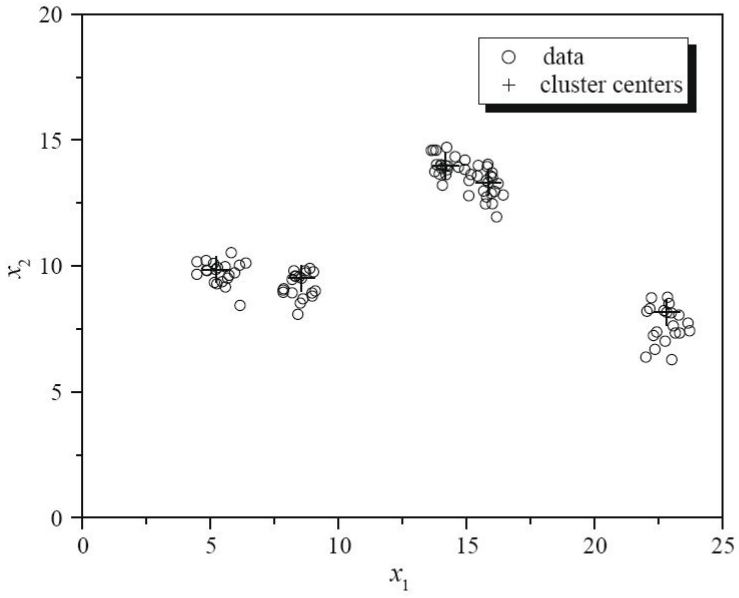


Fig. 6. An example of data clusters and their centers for simple two-dimensional data.

The SC scheme begins by defining a measure of the potential of each data point, which is a function of the Euclidean distances to all other input data points [15]:

$$P_1(k) = \sum_{j=1}^{N} e^{-4\|\mathbf{x}_k - \mathbf{x}_j\|^2 / r_\alpha^2}, \quad k = 1, 2, \cdots, N, \tag{22}$$

where $r_\alpha$ is a radius to define a particular neighborhood of a cluster. Here, it is assumed that N input/output training data $\mathbf{z}_k = (\mathbf{x}_k, y_k)$ are available and the data points are normalized in each dimension. The potential of a data point is defined so that it becomes high when surrounded by many neighboring data. After the potential of each data point is calculated using Eq. (22), the data point with the highest potential is selected as the first cluster center.

In general, after determining the $i$-th cluster center $\boldsymbol{c}_i$ and its potential value $P_i^c$, the potential of each data point is revised using the following equation:

$$\mathrm{P}_{i+1}(k) = \mathrm{P}_i(k) - \mathrm{P}_i^c e^{-4\|\mathbf{x}_k - \mathbf{c}_j\|^2/r_\beta^2}, \quad k = 1, 2, \cdots, N, \tag{23}$$

where $r_\beta$ is usually greater than $r_\alpha$ in order to limit the number of clusters generated. Since an amount of potential is subtracted from each data point as a function of its distance from the former selected cluster center, the data points near to the cluster center have a greatly reduced potential and are unlikely to be selected as the next cluster center.

When the potentials of all data points are recalculated using Eq. (23), the data point with the highest potential is selected as the $(i+1)$th cluster center. The calculation stops if $P_i^c < \epsilon P_i^c$ becomes true, otherwise calculation continues. If the calculation stops finally at an iterative step $N_c$, this means there are $N_c$ cluster centers. The input/output data (training data) positioned in cluster centers are selected to train the SVR model. The remaining data from which the training data set had been eliminated become the test data set.

# Ⅳ. Application to PPF Prediction

The proposed FNN and SVR model were applied to the first fuel cycle of the YGN-3 PWR plant. The used data were obtained [9] by running the MASTER (Multipurpose Analyzer for Static and Transient Effects of Reactor) reactor analysis code [16]. The MASTER code developed by KAERI (Korea Atomic Energy Research Institute) is a nuclear analysis and design program that has a variety of features such as static core design, transient core analysis, and operation support.

## A. Fuzzy Neural Network (FNN)

The data obtained from the simulations of the MASTER code comprise a total of 25,541 input-output data pairs $(x_1, x_2, \cdots, x_{11}, y_r)$. The data are divided into both the training data sets and the test data sets and also, these data sets are divided into two types of data with positive axial shape index (ASI) and negative ASI. $x_1$ through $x_{23}$ represent the reactor power, core inlet temperature, coolant pressure, mass flowrate, axial shape index, 12 in-core neutron sensor signals, R1, R2, R3, R4, R5 and P control rod positions, and $y_r$ is a power peaking factor ($F_q$) in the reactor core. R1 through R5 and P are the names of the control rod groups. The used in-core detector signals are ones located on the central part of the core (a total of 12 in-core sensor signals including instrument locations indicated as instrument numbers 16, 20, 23 and 26 at 3 axial levels in Fig. 7).

The ranges of the input and output signals that are used for training, in this thesis, are described in Table 1. The fuzzy neural networks are trained for two types of data sets divided into both the positive (relatively high power at a top part of a reactor core) ASI cases and the negative ASI cases, which results in smaller errors compared with that of only one summed data set.

The selected number of rules of fuzzy neural networks is 6 for both the positive ASI cases and the negative ASI cases to prevent the underfitting and overfitting problem. The antecedent parameters such as membership function parameters are optimized by the back-propagation method and the consequent parameters $q_{ij}$ and $r$ are optimized by the least-squares method.

Table 1. Input and output signal ranges [9].

| Input signals | Nominal values | Ranges |
|---|---|---|
| Reactor power (%) | 100% | 80 ~ 103 |
| Inlet temperature ($^{o}$C) | 295.8 | 290.5 ~ 301.7 |
| Pressure (bar) | 155.17 | 131.0 ~ 160.0 |
| Mass flowrate (kg/m$^{2}$-sec) | 3565.0 | 2994.6 ~ 4135.4 |
| Axial shape index | - | 0.597 ~ -0.534 |
| R1 control rod positions (cm) | - | 0 ~ 381 |
| R2 control rod positions (cm) | - | 0 ~ 381 |
| R3 control rod positions (cm) | - | 0 ~ 381 |
| R4 control rod positions (cm) | - | 0 ~ 381 |
| R5 control rod positions (cm) | - | 0 ~ 381 |
| P control rod positions (cm) | - | 0 ~ 381 |
| 12 ICI signals (at 4 radial instrument locations and 3 axial levels) | - | 7.4 ~ 322.0 |
| **Output signal** | **Nominal value** | **Range** |
| Power peaking factor | - | 1.930 ~ 4.066 |

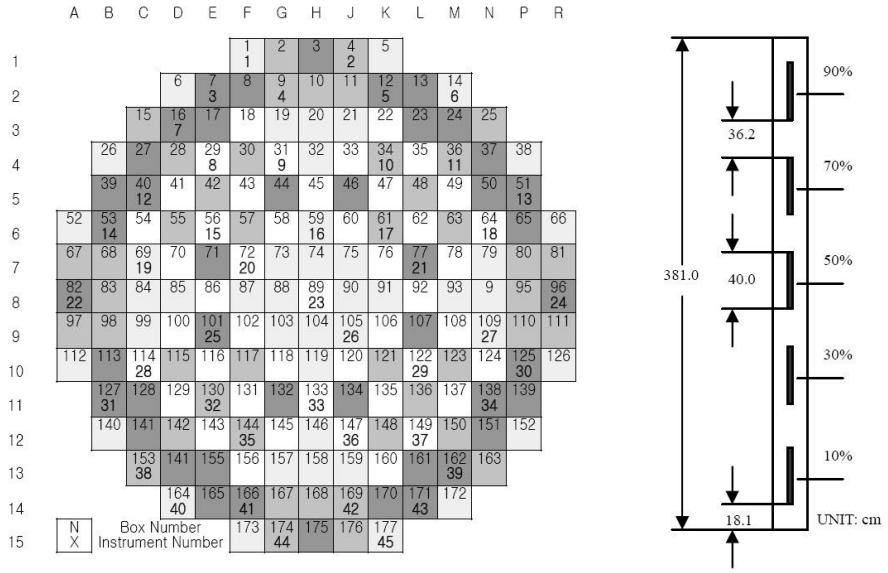


Fig. 7. Fixed rhodium in-core detector location of YGN-3.

## B. Support Vector Regression (SVR)

The data obtained from MASTER simulations comprise a total of 25,541 input-output data pairs; $(x_1, x_2, \cdots, x_{11}, y_r)$ for SVR models without in-core instrument (ICI) signals and $(x_1, x_2, \cdots, x_{23}, y_r)$ for SVR models with ICI signals. The existing monitoring system (COLSS) uses ICI signals, however, the existing protection system (CPCS) does not use the ICI signals because of the slow response of the in-core instruments. Therefore, in this thesis the performances of the proposed SVR model, with and without ICI signals are compared. The data sets are divided into two types of data: those with positive ASI and those with negative ASI. These data sets are then divided into training data sets and test data sets, respectively. The parameters $x_1$ through $x_{11}$ represent respectively the reactor power, core inlet temperature, coolant pressure, mass flow rate, ASI, various control rod bank positions of R1, R2, R3, R4, R5 and P. Also, $x_{12}$ through $x_{23}$ represent, respectively, 12 ICI signals (12 in-core neutron sensor signals at 4 radial instrument locations and 3 axial levels). The parameter $y_r$ is the PPF value of the reactor core.

Ranges of the input and output signals used for training in this thesis are shown in Table 1. Two SVR models are trained for two individual data sets, the positive (relatively high power at the upper part of the reactor core) ASI cases (12,765 cases) and negative ASI cases (12,776 cases). This results in smaller errors compared with using only one general data set.

## C. Application to PPF Prediction

Fig. 8 shows PPF values for 3,351 train cases without ICI signals and the estimation error histogram of the proposed models. In case of FNN, the RMS error is 0.2557% and its maximum error is 1.8599%. Also, note that the RMS error and the maximum error of the SVR model are 0.0604% and 0.5414%, respectively (see Table 2).

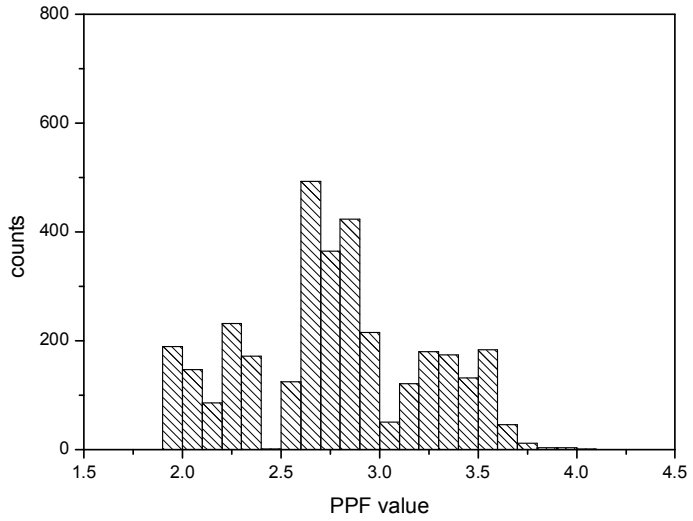


(a) Actual PPF histogram

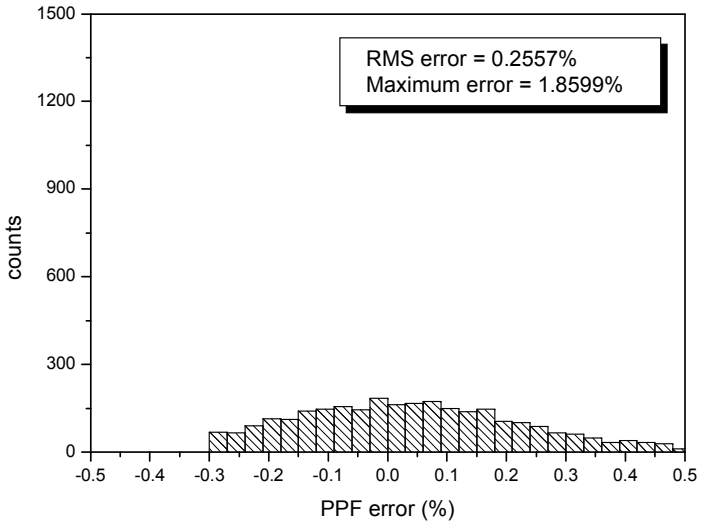


(b) Error histogram between actual PPF and estimated PPF using an FNN model

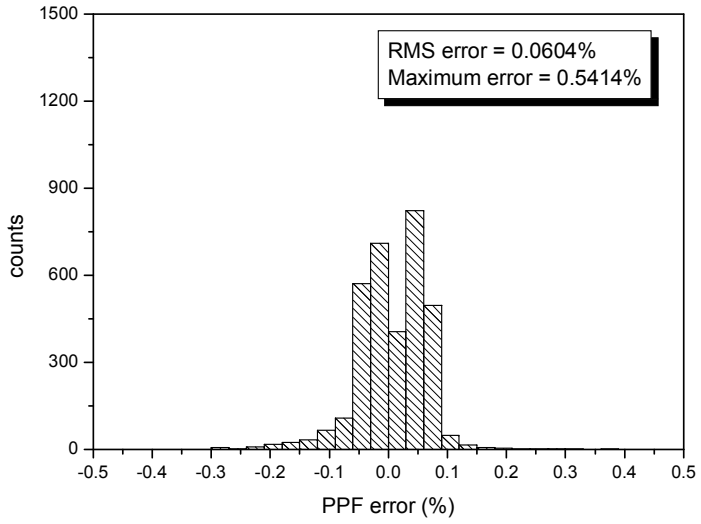


(c) Error histogram between actual PPF and estimated PPF using an SVR model

Fig. 8. Estimation performance of the proposed model without ICI signals for train data.

Table 2. PPF results calculated by the proposed models

| | | | Training data | | | Test data | | |
|---|---|---|---|---|---|---|---|---|
| | | | **Number of data** | **RMS error (%)** | **Relative maximum error (%)** | **Number of data** | **RMS error (%)** | **Relative maximum error (%)** |
| **Proposed model without ICI** | **Positive ASI** | FNN | 1,665 | 0.2889 | 1.8599 | 11,100 | 0.2793 | 1.9061 |
| | | SVR | | **0.0580** | **0.2926** | | **0.0870** | **0.4621** |
| | **Negative ASI** | FNN | 1,686 | 0.2224 | 1.5886 | 11,090 | 0.2088 | **1.5299** |
| | | SVR | | **0.0628** | **0.5414** | | **0.1312** | 1.7624 |
| | **Total** | FNN | 3,351 | 0.2557 | 1.8599 | 22,190 | 0.2441 | 1.9061 |
| | | SVR | | **0.0604** | 0.5414 | | **0.1113** | 1.7624 |
| **Proposed model with ICI** | **Positive ASI** | FNN | 2,119 | 0.1215 | 0.9572 | 10,646 | 0.1507 | 0.9852 |
| | | SVR | | **0.0255** | **0.2029** | | **0.0806** | **0.5504** |
| | **Negative ASI** | FNN | 2,127 | 0.1062 | 0.8464 | 10,649 | 0.1231 | **1.0499** |
| | | SVR | | **0.0835** | **0.3696** | | **0.1106** | 1.3279 |
| | **Total** | FNN | 4,246 | 0.1139 | 0.9572 | 21,295 | 0.1369 | 1.0499 |
| | | SVR | | **0.0618** | 0.3696 | | **0.0968** | 1.3279 |

Fig. 9 shows PPF values for 22,190 test cases without ICI signals and the estimation error histogram of the proposed models. In case of FNN, the RMS error is 0.2441% and its maximum error is 1.9601%. Also, note that the RMS error and the maximum error of the SVR model are 0.1113% and 1.7624%, respectively, which are smaller than those of the FNN model (see Table 2).

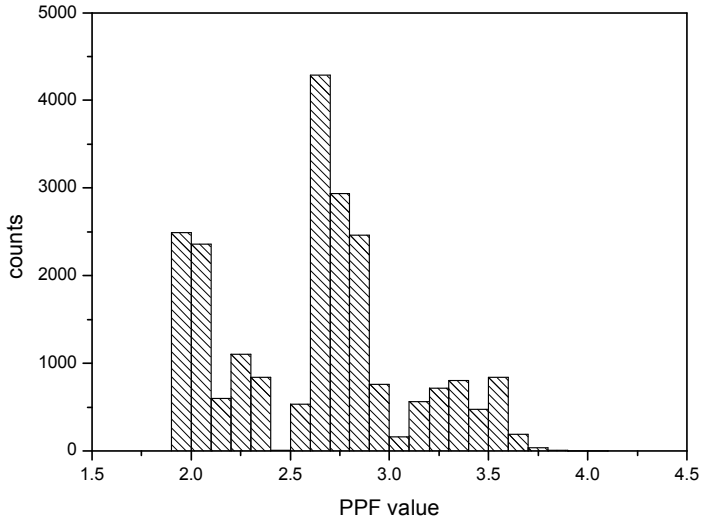


(a) Actual PPF histogram

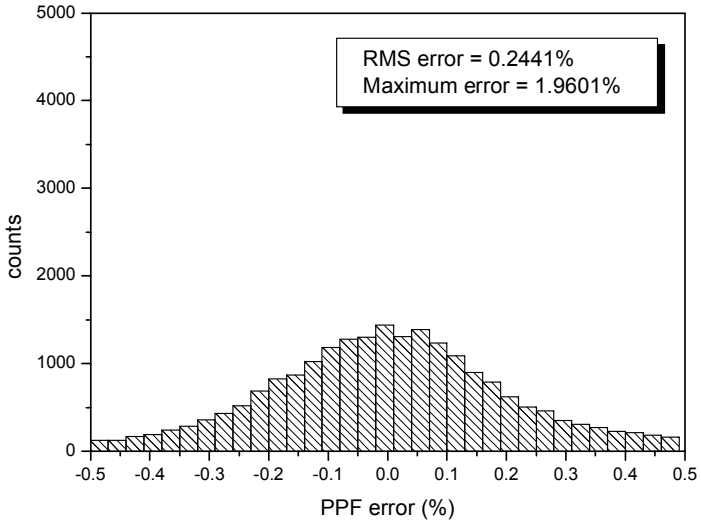


(b) Error histogram between actual PPF and estimated PPF using an FNN model

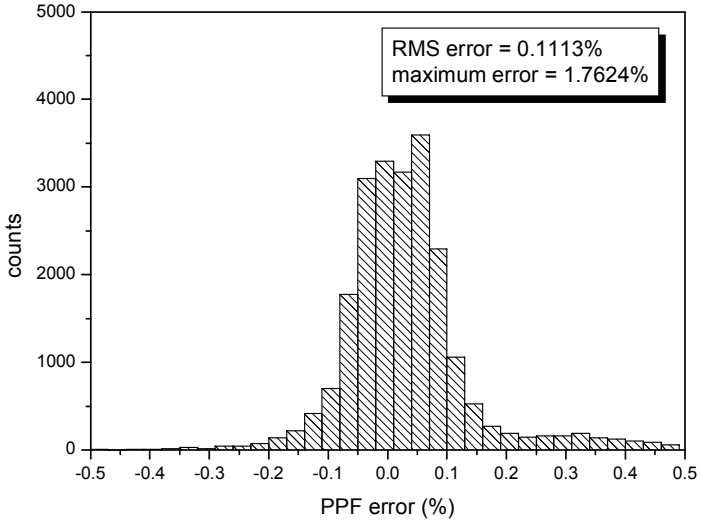


(c) Error histogram between actual PPF and estimated PPF using an SVR model

Fig. 9. Estimation performance of the proposed model without ICI signals for test data.

Fig. 10 shows PPF values for 4,246 train cases with ICI signals and the estimation error histogram of the proposed models. In case of FNN, the RMS error is 0.1139% and its maximum error is 0.9572%. Also, note that the RMS error and the maximum error of the SVR model are 0.0618% and 0.3696%, respectively (see Table 2).

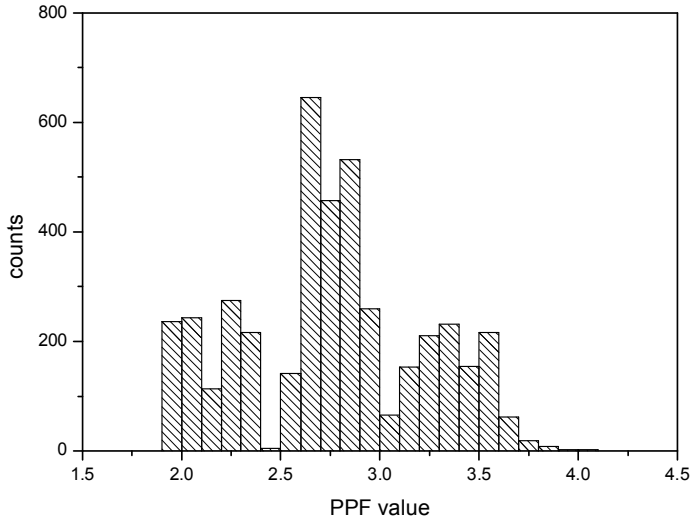


(a) Actual PPF histogram

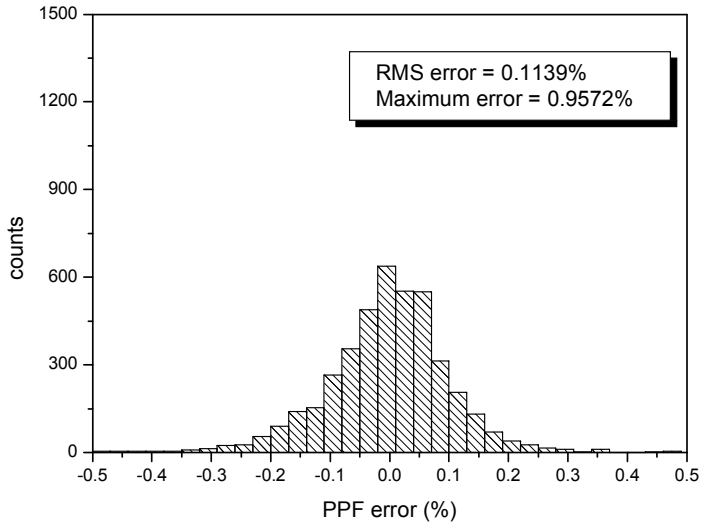


(b) Error histogram between actual PPF and estimated PPF using an FNN model

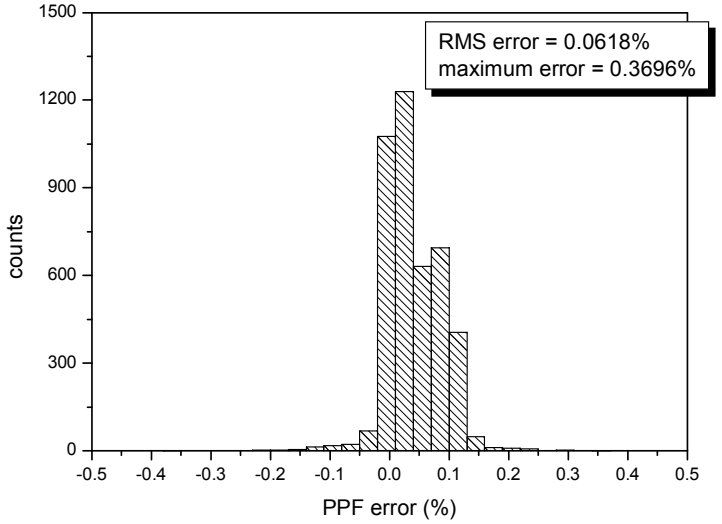


(c) Error histogram between actual PPF and estimated PPF using an SVR model

Fig. 10. Estimation performance of the proposed model with ICI signals for train data.

Fig. 11 shows the PPF values for 21,295 test cases with ICI signals and the estimation error histogram of the proposed models. The RMS error of the proposed FNN model is 0.1369% and its maximum error is 1.0499%. Also, note that the RMS error and the maximum error of the SVR model are 0.0968% and 1.3279%, respectively, which are smaller than those of the FNN model (see Table 2).

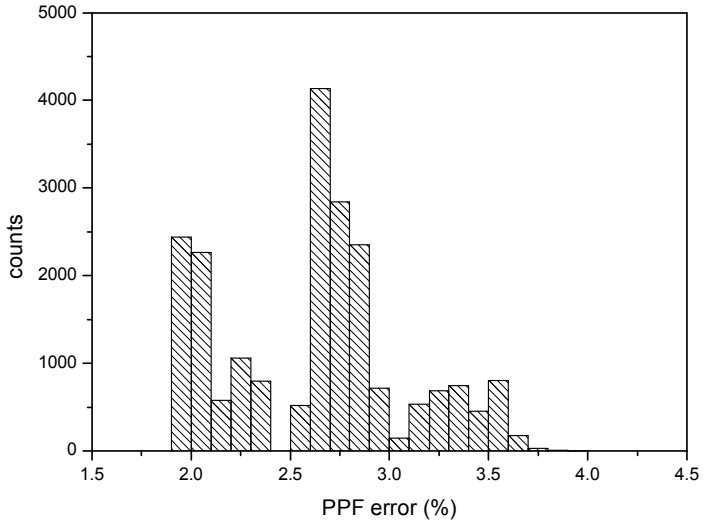


(a) Actual PPF histogram

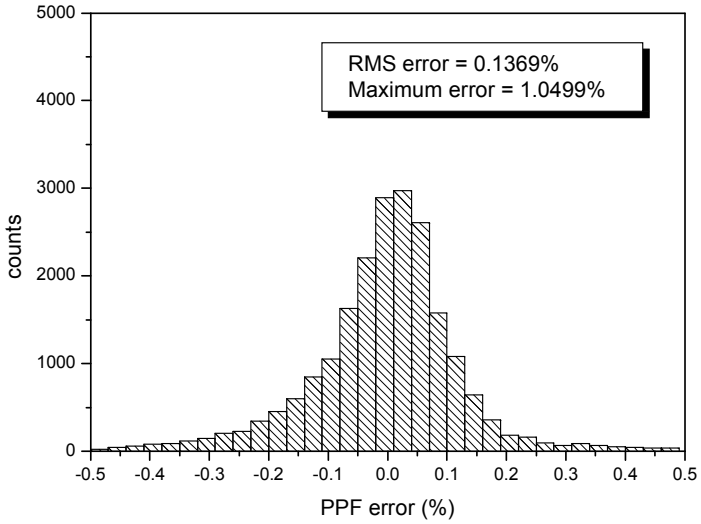


(b) Error histogram between actual PPF and estimated PPF using an FNN model

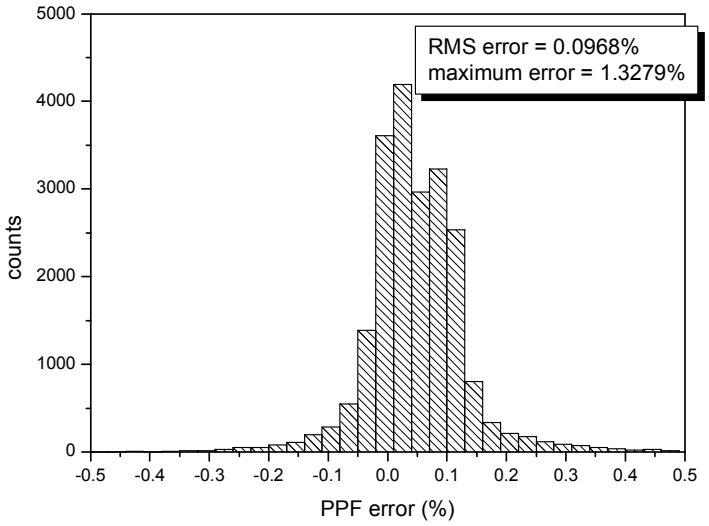


(c) Error histogram between actual PPF and estimated PPF using an SVR model

Fig. 11. Estimation performance of the proposed model with ICI signals for test data.

Table 3 shows the effect of training data selection methods; SC scheme and fixed interval scheme. The fixed interval scheme selects the training data every fixed interval. It is shown that the SC scheme can improve the performance of the SVR model. RMS error of the SC scheme is 0.0618% for the train data, whereas that of the fixed interval scheme is 0.0847%. Also, RMS error of the SC scheme is 0.0968% for the test data, whereas that of the fixed interval scheme is 0.1363%.

Table 3. Effect of training data selection

| Selection methods of training data | Sign of ASI values | Training data | | | Test data | | |
|---|---|---|---|---|---|---|---|
| | | Number of data | RMS error (%) | Relative maximum error (%) | Number of data | RMS error (%) | Relative maximum error (%) |
| SC scheme (With ICI) | Positive ASI | 2,119 | 0.0255 | 0.2029 | 10,646 | 0.0806 | 0.5504 |
| | Negative ASI | 2,127 | 0.0835 | 0.3696 | 10,649 | 0.1106 | 1.3279 |
| | Total | 4,246 | 0.0618 | 0.3696 | 21,295 | 0.0968 | 1.3279 |
| Fixed interval scheme (With ICI) | Positive ASI | 2,119 | 0.0933 | 0.2158 | 10,646 | 0.1410 | 5.4332 |
| | Negative ASI | 2,127 | 0.0751 | 0.3033 | 10,649 | 0.1315 | 5.4731 |
| | Total | 4,246 | 0.0847 | 0.3033 | 21,295 | 0.1363 | 5.4731 |

Table 4 shows other test results to compare PPF values with the existing COLSS methodology [9]. The $F_q$ values calculated by the COLSS method are obtained by multiplying the core average axial power $P1D(z)$ to the $F_{xy}$ values of the corresponding regions and then by selecting its maximum (refer to Fig. 12). Here, $z$ denotes the axial position of a reactor core and $F_{xy}$ is a plane-wise (radial direction) peaking factor. In the COLSS method, the $F_{xy}$ values are prepared and provided at a design stage according to a variety of the control rod configurations. For example, for the control rod configurations of Fig. 12, each $F_{xy}$ for 3 different regions is selected by a table lookup scheme from the $F_{xy}$ values prepared at a design stage. But in the MASTER code the plane-wise $F_{xy}$ values at the real core state are used to calculate the $F_q$ value. Therefore, if the proposed models accurately estimate the target $F_q$ values, the proposed method always provides the less or equal $F_q$ value than that of COLSS method, and the COLSS method is always equally or excessively conservative than the proposed methods.

The rightmost values in Table 4 are PPFs calculated under the assumption that all 12 incore sensor signals are over-measured by 5% compared to actual values. The ICI signals have measurement error that can be under-estimated or over-estimated. The assumption that all 12 ICI signals are over-measured by 5% is severe with respect to increasing PPF (reducing safety). Even PPFs for these severe cases are lower than those of COLSS. Thus, the proposed methods secure larger operation margin than the existing COLSS.

Table 4. Comparison of calculated PPFs.

| ASI value | Power | MASTER (target) | Proposed model (without ICI) | | Proposed model (with ICI) | | COLSS | Proposed model (with ICI)[1)] | |
|---|---|---|---|---|---|---|---|---|---|
| | | | FNN | SVR | FNN | SVR | | FNN | SVR |
| 0.081 | 80 | 1.968 | 1.967 | 1.966 | 1.974 | 1.965 | 2.133 | 2.051 | 2.013 |
| 0.094 | 90 | 1.959 | 1.957 | 1.958 | 1.962 | 1.955 | 2.135 | 2.050 | 2.009 |
| 0.069 | 100 | 1.952 | 1.953 | 1.952 | 1.954 | 1.952 | 2.137 | 2.055 | 1.998 |
| 0.073 | 103 | 1.949 | 1.950 | 1.950 | 1.953 | 1.951 | 2.138 | 2.058 | 1.996 |
| -0.525 | 80 | 2.778 | 2.774 | 2.777 | 2.774 | 2.776 | 3.000 | 2.915 | 2.804 |
| -0.504 | 90 | 2.718 | 2.725 | 2.718 | 2.717 | 2.716 | 2.961 | 2.881 | 2.741 |
| -0.483 | 100 | 2.663 | 2.670 | 2.663 | 2.664 | 2.660 | 2.918 | 2.852 | 2.691 |
| -0.520 | 103 | 2.646 | 2.652 | 2.647 | 2.650 | 2.642 | 2.905 | 2.845 | 2.681 |

[1)] Values calculated under the assumption that all 12 ICI signals are over-measured 5% more largely than actual values

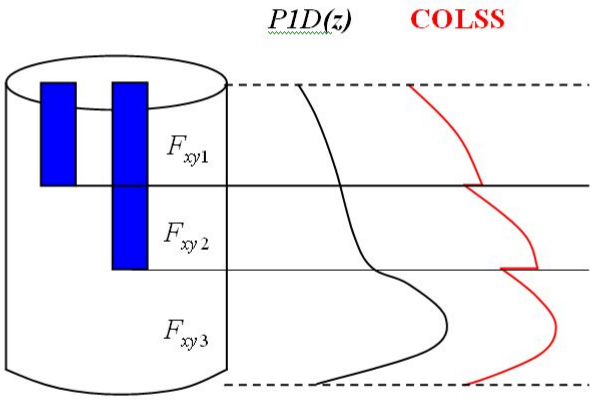


Fig. 12. The pseudo hot pin axial power distribution of COLSS.

# Ⅴ. Conclusions

In this thesis, a fuzzy neural network (FNN) and a support vector regression (SVR) models have been developed to correctly predict the power peaking factor in a nuclear reactor core.

In this study, the proposed models have been developed and applied to the estimation of the PPF in the reactor core. The proposed models are trained by using the data set prepared for training (training data) and verified by using a different data (test data) set. The developed models are trained for two types of data sets divided into both the positive ASI and the negative ASI, respectively. The training data are selected by an SC scheme. It was known that this could improve the performance of the SVR models. The developed FNN and SVR models were applied to the first fuel cycle of the YGN-3.

The RMS error of the estimated PPF is 0.2441% for the FNN model without ICI signals and 0.1369% for the FNN model with ICI signals. In case of SVR model, the RMS error of the estimated PPF is 0.1113% without ICI signals and 0.0968% with ICI signals. And also, the use of ICI signals as input signals to the proposed algorithms reduces the estimation error compared to that not using the ICI signals. In case of FNN, the use of ICI signals as input signals reduces the estimation error about two times compared to that not using the ICI signals. In summary, the proposed models are sufficiently accurate for using in power peaking factor monitoring. And also, the estimation performance of SVR models is superior to the estimation performance of FNN.

Consequently, we could confirm that the performance of the SVR models is superior to any other method. Therefore, it is expected that this model can be applied to predict reactor core power peaking factor.

# References

[1] ABB Combustion Engineering Inc., Overview Description of the Core Operation Limit Supervisory System (COLSS). CEN-312-P, Revision 01-P. (1986)

[2] Kim, H.C., Chang, S.H., Development of a back propagation network for onestep transient DNBR calculations. *Annals of Nuclear Energy* 24, 1437–.1446. (1997)

[3] Lee, J.K., Han, B.S., Modeling of core protection and monitoring system for PWR nuclear power plant simulator. *Annals of Nuclear Energy* 25, 409–.420. (1998)

[4] Han, S., Kim, U.S., Seong, P.H., A methodology for benefit assessment of using in-core neutron detector signals in core protection calculator system (CPCS) for Korea standard nuclear power plants (KSNPP). *Annals of Nuclear Energy* 26, 471–.488. (1999)

[5] Na, M.G., Application of a genetic neuro-fuzzy logic to departure from nucleate boiling protection limit estimation. *Nuclear Technology* 128, 327–.340. (1999)

[6] Na, M.G., DNB limit estimation using an adaptive fuzzy inference system. *IEEE Transactions on Nuclear Science* 47, 1948–.1953. (2000)

[7] In, W.K., Hwang, D.H., Yoo, Y.J., Zee, S.Q., Assessment of core protection and monitoring systems for an advanced reactor MART. *Annals of Nuclear Energy* 29, 609–.621. (2002)

[8] Lee, G.C., Baek, W.P., Chang, S.H., Improved methodology for generation of axial flux shapes in digital core protection systems. *Annals of Nuclear Energy* 29, 805–.819. (2002)

[9] Na, M.G., Jung, D.W., Shin, S.H., Lee, K.B., Lee, Y.J., Estimation of the nuclear power peaking factor using in-core sensor signals. *Nuclear Engineering and Technology* 36, 420–.429. (2004)

[10] Vapnik, V.N., Statistical Learning Theory. John Wiley & Sons. (1998)

[11] Gunn, S.R., Support Vector Machines for Classification and Regression. Technical Report, University of Southampton. (1998)

[12] Kecman, V., Learning and Soft Computing. MIT Press. (2001)

[13] Na, M.G., Hwang, I.J., Lee, Y.J., Inferential sensing and monitoring for feedwater flowrate in pressurized water reactors. *IEEE Transactions on Nuclear Science* 53, 2335–342. (2006)

[14] I.V. Tetko, D.J. Livingstone, A.I. Luik, "Neural Network Studies. 1. Comparion of Overfitting and Overtraining," *J. Chem. Inf. Comput. Sci.*, Vol. 35, No. 5, pp. 826-833 (1995).

[15] Chiu, S.L., Fuzzy model identification based on cluster estimation. *Journal of Intelligent and Fuzzy Systems 2*, 267–78. (1994)

[16] Cho, B.O., et al. MASTER-2.0: Multi-purpose analyzer for static and transient (1999)

# 감사의 글

16층! 조선대학교 공과대학 제 1 공학관에서 꼭대기 아래층에 자리 잡고 있는 실험실... 매일 아침마다 '오늘은 이것 이것을 해야지' 거창하지도 않은 계획을 세우지만 하루일과를 마치고 실험실을 나갈 때면 무엇인가 허전하다.

아침마다 실험실원들과 인사를 나누곤 모두들 바쁜 일상 속으로 접어들지만 서로를 위하는 마음만은 가득하였었던 공간이었던 듯하다.

헌영이... 같은 해에 "원자력공학과 신입생 ○○○입니다!" 외치던 때가 엊그제 같은데 벌써 함께 졸업이라니... 언제나 나에게 힘을 실어주었던 동기. 학부 동기로서 대학원 선배로서 나에게 많은 것을 알려주고 배려해 주었던 헌영이에게 항상 고마운 마음이 가득하다.

동혁이... 나에겐 학부 후배이지만 항상 '동혁이가 나의 후배인가?' 이런 의구심을 갖고 살았을 만큼이나 나에게 항상 쓴소리와 단소리를 적절하게 해주어서 자극을 시켜주고 나에게 아드레날린을 주입시켜 주었던 친구. 굳이 말을 하지 않아도 마음을 알아주었던 동혁이가 있어 더욱 잘 지낼 수 있었던 것 같다.

나의 지도교수님이신 나 만균 교수님!

2005년 아무것도 검증되지 않은 저를 저의 욕심 하나로 찾아뵈었을 때 흔쾌히 저에게 실험실 책상 하나를 내어 주셨던 평생지도 교수님. 첫 발표 때가 생각납니다. 발표경험이 부족한 저에게 따뜻한 격려와 용기와 충고를 아끼지 않고 해주셔서 생각해보면 지금은 그때 보다 더욱 발전한 저의 모습을 발견 할 수 있습니다. 항상 실험실원들에게 '열 손가락 깨물어 안 아픈 손가락이 어디 있을까?' 이 명언을 몸소 실천해 주시고 교수님 이하 제자들에게 조금이나마 더 많은 경험을 쌓게 해 주시기 위해 지원과 응원을 아끼지 않아 주셔서 항상 감사하게 생각합니다. 평생의 선생님으로 자리

잡으신 스승님. 감사하고 사랑합니다.

이제까지 아들 말 한 마디만을 믿고 지원과 믿음의 줄을 놓지 않으시고 지켜봐 주신 아버지, 어머니! 부모님 말씀처럼 씨앗을 뿌렸으니 거둬들일 준비를 해야 할 시기가 되었습니다. 더 큰 곳을 바라보며 달려 왔었던 지난 2년 이라는 시간동안 가장 커다란 힘을 주셨던 분들은 바로 부모님! 아버지! 어머니!입니다. 무슨 말이 더 필요하겠습니까? 감사하고 사랑합니다. 아버지, 어머니.

먼 타국 스리랑카에서 고생하는 상영이... 1년에 두 번밖에 얼굴을 마주 할 순 없지만 항상 나를 먼저 걱정해주고 격려해주는 지음(知音)이라는 존재로 나의 곁에 머물러 주는 친구.

그리고 2년이라는 시간을 함께 해준 실험실원 성한, 동수, 심원에게 고맙다.

마지막으로 *Sunny!*

3년이라는 짧지만은 않은 시간동안 나의 곁에서 묵묵히 나의 마음이 흔들리거나 아프거나 기쁠 때 항상 힘이 되어주고 버팀목이 되어 주었던 바위에 뿌리를 내린 소나무 같은 친구. 네가 없었다면 이 먼 길까지 오지 못했을지도 모르겠다. 많은 것을 해주지 못하여서 항상 미안한 마음뿐이지만  써니 덕분에 더욱 성장 할 수 있었던 지난 2년이었다. 사랑하고 또 사랑한다.

여기에 이름을 올리진 못 했지만 주위의 수많은 지인들에게 미안하고 고마운 마음뿐이고 더 성장한 내가 되고 항상 노력하는 '仁皓'가 되길...

2009년 05월

조선대학교 원자력공학과 원전계측제어 실험실 배 인 호

# 저작물 이용 허락

| 학 과 | 원자력공학과 | 학 번 | 20087106 | 과 정 | 석사 |
|---|---|---|---|---|---|
| 성 명 | 한글: 배 인 호 한문 : 裵 仁 皓 영문 : Bae In-Ho | | | | |
| 주 소 | 광주광역시 광산구 우산동 우미아파트 103동 1202호 | | | | |
| 연락처 | E-MAIL : blue2106@hotmail.com | | | | |
| 논문제목 | 한글 : 인공지능을 이용한 원자로 출력첨두치 예측 | | | | |
| | 영문 : Prediction of a Reactor Core Power Peaking Factor Using Artificial Intelligence | | | | |

본인이 저작한 위의 저작물에 대하여 다음과 같은 조건아래 조선대학교가 저작물을 이용할 수 있도록 허락하고 동의합니다.

- 다 음 -

1. 저작물의 DB구축 및 인터넷을 포함한 정보통신망에의 공개를 위한 저작물의 복제, 기억장치에의 저장, 전송 등을 허락함
2. 위의 목적을 위하여 필요한 범위 내에서의 편집·형식상의 변경을 허락함. 다만, 저작물의 내용변경은 금지함.
3. 배포·전송된 저작물의 영리적 목적을 위한 복제, 저장, 전송 등은 금지함.
4. 저작물에 대한 이용기간은 5년으로 하고, 기간종료 3개월 이내에 별도의 의사 표시가 없을 경우에는 저작물의 이용기간을 계속 연장함.
5. 해당 저작물의 저작권을 타인에게 양도하거나 또는 출판을 허락을 하였을 경우에는 1개월 이내에 대학에 이를 통보함.
6. 조선대학교는 저작물의 이용허락 이후 해당 저작물로 인하여 발생하는 타인에 의한 권리 침해에 대하여 일체의 법적 책임을 지지 않음
7. 소속대학의 협정기관에 저작물의 제공 및 인터넷 등 정보통신망을 이용한 저작물의 전송·출력을 허락함.

**동의여부 : 동의( ○ ) 반대( )**

2009년 5월 일

저작자: 배 인 호 (서명 또는 인)

## 조선대학교 총장 귀하